Lean, but not obese, fat is enriched for a unique population of regulatory T cells that affect metabolic parameters

Markus Feuerer[1,5], Laura Herrero[2,5], Daniela Cipolletta[1,4,5], Afia Naaz[2], Jamie Wong[1,5], Ali Nayer[2], Jongsoon Lee[2], Allison B Goldfine[3], Christophe Benoist[1,5], Steven Shoelson[2] & Diane Mathis[1,5]

Obesity is accompanied by chronic, low-grade inflammation of adipose tissue, which promotes insulin resistance and type-2 diabetes. These findings raise the question of how fat inflammation can escape the powerful armamentarium of cells and molecules normally responsible for guarding against a runaway immune response. CD4+ Foxp3+ T regulatory (Treg) cells with a unique phenotype were highly enriched in the abdominal fat of normal mice, but their numbers were strikingly and specifically reduced at this site in insulin-resistant models of obesity. Loss-of-function and gain-of-function experiments revealed that these Treg cells influenced the inflammatory state of adipose tissue and, thus, insulin resistance. Cytokines differentially synthesized by fat-resident regulatory and conventional T cells directly affected the synthesis of inflammatory mediators and glucose uptake by cultured adipocytes. These observations suggest that harnessing the anti-inflammatory properties of Treg cells to inhibit elements of the metabolic syndrome may have therapeutic potential.

Type 2 diabetes and other elements of the metabolic syndrome have increased at an alarming rate over the past several decades. There has been a parallel rise in the incidence of obesity, now recognized to be a major contributor to the insulin resistance underlying this spectrum of metabolic abnormalities[1]. Just how obesity promotes insulin resistance is still unclear, but results from clinical, epidemiological and molecular studies have converged to highlight the role of inflammation[1].

Prolonged nutrient overload results in a state of chronic, low-grade inflammation in adipose tissue[2] and systemically[3], particularly in visceral fat depots[4]. Visceral fat produces a number of inflammatory cytokines and chemokines (such as leptin, tumor necrosis factor-α (TNF-α), macrophage chemoattractant protein-1 and interleukin-6 (IL-6), among others), whose production can be pathologically dysregulated in the obese state, contributing in an important manner to insulin resistance[5].

At the cellular level, macrophages have a key role. With increasing obesity, they accumulate in visceral fat tissue, sometimes contributing as much as half of the cellularity[6,7]. The increase in number is accompanied by an evolution in phenotype from the anti-inflammatory (or 'alternatively activated') M2 form to the proinflammatory (or 'classically activated') M1 form[8,9], which correlates with an increase in insulin resistance (for example, see ref. 10). In the obese state, macrophages and adipocytes make several of the same inflammatory regulators and mediators, including TNF-α, IL-6, matrix metallopro-

teinases (MMPs), peroxisome proliferator activated receptor-γ and fatty acid–binding protein-4 (reviewed in refs. 1,11). These findings, along with others, suggest that adipocytes and adipose-tissue macrophages may contribute to insulin resistance in concert, both inhibiting and enhancing each other's activities[11].

Like any inflammatory state, the chronic, low-grade inflammation associated with obesity should be subject to the control mechanisms that normally curb overactive immune responses. These mechanisms encompass a number of cell types, which can operate through cell-cell contact via a variety of receptors, or through a diversity of soluble mediators. Cells with a potentially regulatory phenotype have previously been associated with obesity (for example, natural killer T cells)[12], and there have been previous reports of anti-inflammatory cytokines being detected in adipose tissue (for example, IL-10 and transforming growth factor-β (TGF-β))[8,9]. Yet, research on this topic has been quite limited, and the influence—or loss of influence—of major control mechanisms remains unaddressed. For example, the role of arguably the most potent regulatory cell population, CD4+Foxp3+ Treg cells, has yet to be explored.

Treg cells, a small subset of T lymphocytes, normally constituting only 5–20% of the CD4+ compartment, are thought to be one of the body's most crucial defenses against inappropriate immune responses, operating in contexts of autoimmunity, allergy, inflammation, infection and tumorigenesis[13,14]. Typically, they control the behavior of
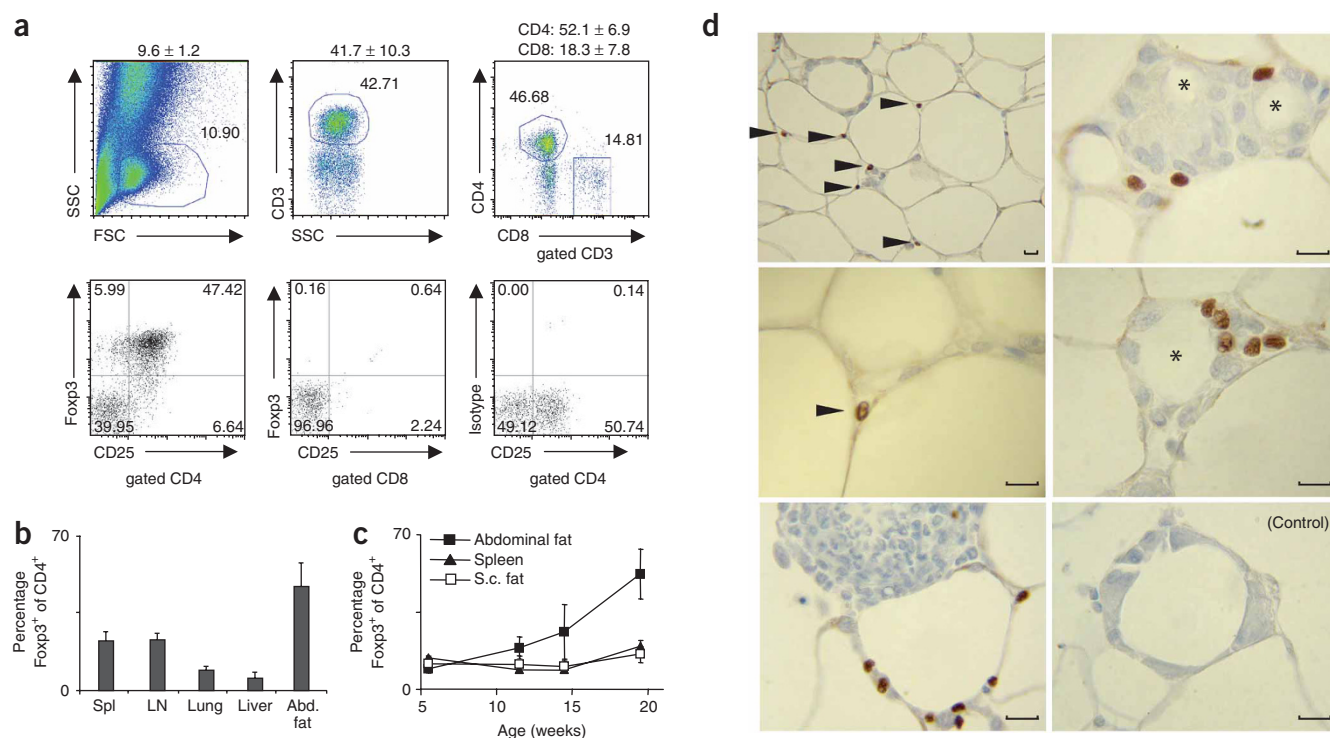
Figure 1 Abdominal (epididymal) and subcutaneous fat pads as well as spleen, lymph node, lung and liver were isolated from retired-breeder B6 male mice, and the stromovascular fraction was stained for Foxp3, CD3, CD4, CD8 and CD25. (**a**) Top, T cell distribution in stromovascular fraction from abdominal fat tissue. Numbers on top indicate the mean ± s.d. from six experiments for cells in the lymphocyte gate (left), fraction of CD3$^+$ T cells among lymphocyte-gated cells (center) and distribution of CD4$^+$ and CD8$^+$ T cells (right). Bottom, percentage of Foxp3$^+$CD25$^+$ T cells in abdominal fat tissue gated on CD4$^+$ (left) or CD8$^+$ (center) T cells. Organs of five mice were pooled. Representative dot plots are shown. FSC, forward scatter; SSC, side scatter. Numbers on the graphs indicate the percentage of cells in that gate for that particular experiment. (**b**) Frequency of Foxp3$^+$ T cells among CD4$^+$ cells in different organs. Means ± s.d. from at least three independent experiments are shown, and organs from four or five mice per experiment were pooled. Spl, spleen; LN, lymph node. (**c**) Kinetics of T$_{reg}$ cell appearance in abdominal and subcutaneous (s.c.) fat tissue as well as in spleen. Error bars represent mean ± s.d. (**d**) Immunohistology of abdominal adipose tissue. Arrowhead indicates Foxp3 staining. Foxp3 expression is restricted to the nucleus. Asterisks refer to dead adipocyte residue surrounded by a crown-like structure formed by immune cells. Control staining is with isotype antibody. Original magnification: top left, 400×; all others, 1000×.

other T cell populations, but they can also influence the activities of cells of the innate immune system[15–17]. T$_{reg}$ cells are characterized by expression of the forkhead–winged-helix transcription factor, Foxp3. Deficiencies in this factor cause the lymphoproliferation and multiorgan autoimmunity found in scurfy mutant mice and humans with immunodysregulation polyendocrinopathy enteropathy X-linked syndrome.

Here we examined the T$_{reg}$ cells residing in mouse adipose tissue with regards to both their proportion and phenotype in visceral versus subcutaneous fat depots in lean versus obese mice. We evaluated their functional importance in loss-of-function, gain-of-function and *in vitro* experiments. Lastly, we sought an analogous population in human adipose tissue samples. Our observations identify a unique fat-resident T lymphocyte population whose products may have applications in treating the metabolic syndrome.

RESULTS
Adipose tissue T$_{reg}$ cells

Adipose tissue is composed of multiple cell types. Most prominent are adipocytes, but vascular endothelial cells, macrophages[6,7] and lymphocytes[12,18] are also found in the stromovascular fraction. According to multiparameter flow cytometry, about 10% of the cells in the stromovascular fraction of abdominal fat from ~30-week-old C57BL/6 (B6) mice fell within the lymphocyte gate (**Fig. 1a**). Close to half of the cells in this gate were of the CD3$^+$ T lineage, split 3:1 between the

CD4$^+$ and CD8$^+$ compartments, respectively (**Fig. 1a**). To our surprise, more than half of the CD4$^+$ T cells expressed Foxp3 (**Fig. 1a**), a much higher fraction than that normally found in lymphoid (for example, in the spleen or lymph nodes) or nonlymphoid (for example, lung or liver) tissues (**Fig. 1b**), including in subcutaneous fat (**Fig. 1c**). Visceral and subcutaneous adipose tissue had similar low fractions of T$_{reg}$ cells at birth, with a progressive accumulation over time in the visceral, though not the subcutaneous, depot (**Fig. 1c**). This dichotomy in T$_{reg}$ cell accumulation between these two fat depots is potentially crucial, given the association of visceral, but not subcutaneous, fat with insulin resistance[4,19].

Immunohistological examination revealed Foxp3$^+$ cells in the spaces between adipocytes, mainly, but not only, in regions where several of them intersected (**Fig. 1d**). Fat tissue, especially from obese individuals, can host substantial numbers of macrophages, which accumulate in so-called 'crown-like' structures that are replete with dead adipocyte residues[6,7,20]. We observed T$_{reg}$ cells in such structures, in close proximity to macrophages and other leukocyte aggregates (**Fig. 1d**). We estimate that 15,000–20,000 Foxp3$^+$ cells reside in 1 g of epididymal adipose tissue in an ~30-week-old B6 mouse.

Expression profiling of fat T$_{reg}$ cells reveals a unique phenotype

We next addressed whether the CD25$^+$Foxp3$^+$ cells in abdominal adipose tissue were of the typical T$_{reg}$ phenotype (**Fig. 2**). They functioned as effectively as analogous cells isolated from the spleen

when introduced into a standard *in vitro* suppression assay (**Fig. 2a**). Fat-resident T conventional (T_conv) cells also performed as expected; that is, they had no suppressive activity and had a normal proliferative response (**Fig. 2a**). The lability and low recoverable numbers of fat-resident T_reg cells have so far prevented us from assaying their activities in *in vivo* suppressor assays. So we turned to the well-established transcriptional T_reg cell signature, derived from the data of multiple groups[21–24], as an indicator of *in vivo* function.

The overall transcript profile of the T_reg cell population from visceral fat differed from the patterns of its spleen and lymph node counterparts more than the latter two did from each other (**Fig. 2b**). This observation also held for the T_conv cell populations at these sites, though not as notably so (**Fig. 2c**). Focusing specifically on the documented T_reg cell signature[21–24], we found that our data from the spleen showed an excellent recapitulation of its major features; as anticipated, most genes known to be upregulated in T_reg cells descended to the right on the *P* value versus fold change 'volcano' plot, whereas most downregulated loci dropped to the left (**Fig. 2d**). Fully 93% of the signature was present. In contrast, evidenced by their position at the volcano summit, many of the signature T_reg cell genes were not significantly up- or downregulated in the corresponding population from visceral fat (for example, CD103 and G protein–coupled receptor-83) (**Fig. 2d**). We confirmed the

data on CD103 by flow cytometric analysis (**Fig. 3**). These observations on the T_reg cell signature were true whether the comparator was T_conv cells from the fat or the lymph node (**Fig. 2d**), arguing that they reflect special features of adipose tissue T_reg cells. Nonetheless, the fat-resident CD4$^+$Foxp3$^+$ cells were clearly T_reg cells, as much (63%) of the signature was intact, including overexpression of hallmark transcripts such as those encoding CD25, glucocorticoid-induced tumor necrosis factor receptor (GITR), cytotoxic T lymphocyte antigen-4 (CTLA-4), OX40 and killer cell lectin-like receptor G1, in addition to Foxp3 itself (**Figs. 2 and 3**). We confirmed the elevated expression of several of these signature genes in fat T_reg cells by RT-PCR and flow cytometric
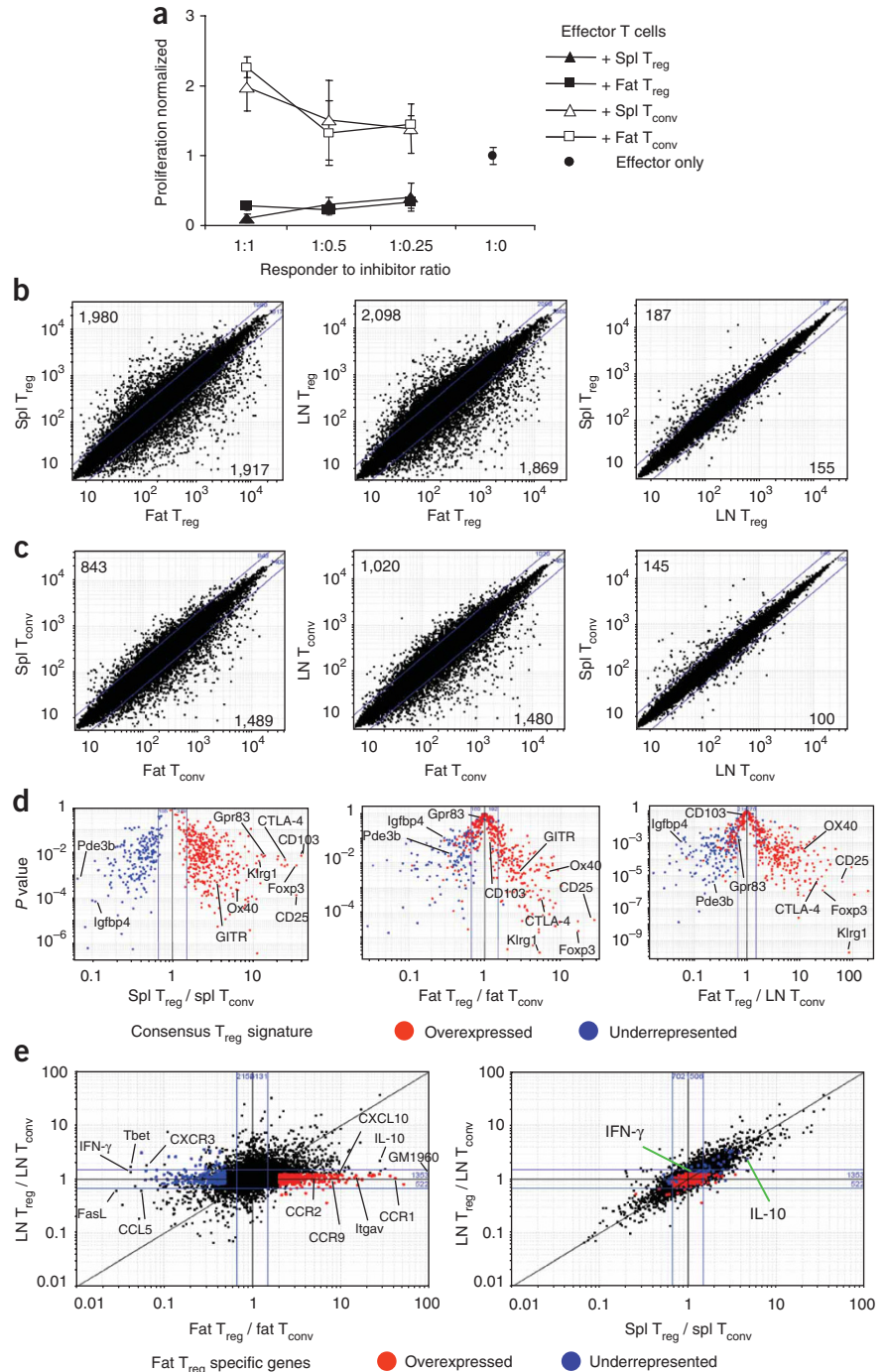

Figure 2 Functional comparison of T_reg and T_conv cells from abdominal adipose tissue, lymph node and spleen. CD4$^+$CD25$^+$ T_reg and T_conv cells were isolated from retired-breeder B6 mice. (**a**) A standard *in vitro* suppression assay. Spleen-derived CD4$^+$ effector T cells (responder cells) were incubated at various ratios with different T cell populations (Fat: adipose tissue-derived T cells). (**b–e**) Analysis with Affymetrix microarray chips. Normalized expression values for profiles directly comparing T_reg cells (**b**) in fat versus spleen (left), fat versus lymph node (center) and lymph node versus spleen (right) or for profiles directly comparing T_conv cells (**c**) in fat versus spleen (left), fat versus lymph node (center) or lymph node versus spleen (right). The numbers in **b** and **c** indicate the number of genes whose expression differed by more or less than twofold. (**d**) Volcano plots of gene expression data comparing *P* value versus fold change for probes from the consensus T_reg cell signature[21,24], plotted for spleen T_reg cells versus T_conv cells (left), fat T_reg cells versus T_conv cells (center); fat T_reg cells versus lymph node T_conv cells (right). The color coding in the figures denotes genes 1.5-fold over- (red) or under- (blue) expressed in T_reg cells in all four reference data sets. (**e**) Fold change versus fold change plots comparing T_reg expression profiles between fat T_reg cells (*x* axis) and lymph node T_reg cells (*y* axis) (left) and spleen T_reg cells (*x* axis) and lymph node T_reg cells (*y* axis) (right). Gene transcripts uniquely up- or downregulated in fat T_reg cells are highlighted in red and blue, respectively.
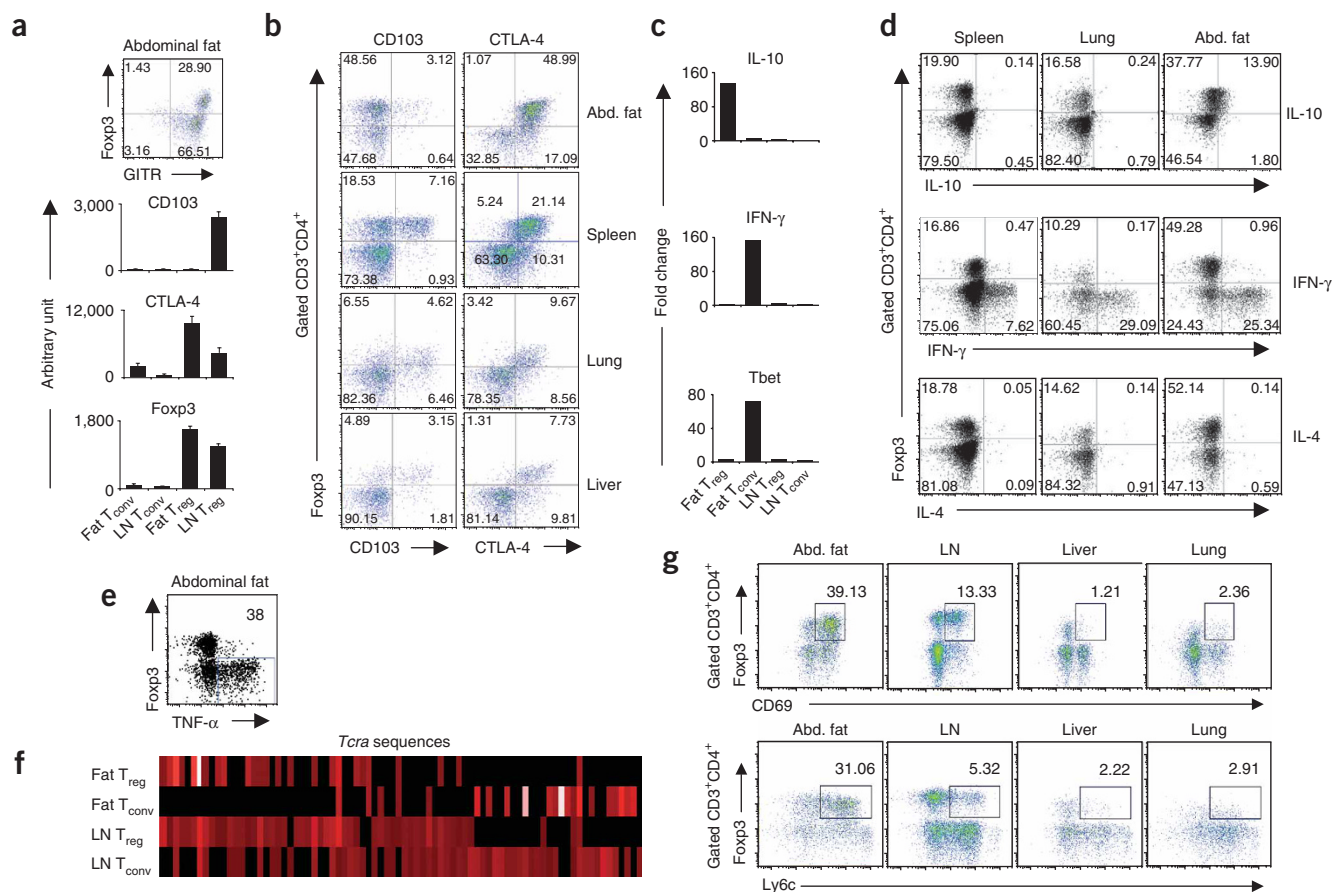
Figure 3 Phenotypic characterization of T_{reg} cells from abdominal fat tissue, spleen, lung and liver. (**a,b**) Cells were isolated from retired-breeder B6 mice, and the stromovascular fraction was stained for Foxp3, CD3, CD4, CD8, CD25, glucocorticoid-induced tumor necrosis factor receptor (GITR), CD103 and CTLA-4. Numbers on the graph indicate the percentage of cells in that gate for that particular experiment. (**a,c**) Relative RNA expression of selected genes from T_{reg} and T_{conv} cells from lymph node and fat. Error bars represent means ± s.d. (**d,e**) Cytokine expression profile from T_{reg} and T_{conv} cells from spleen, lung and fat tissue. Representative dot plots of at least three independent experiments are shown. Organs from four to six mice were pooled per experiment. Numbers on the graph indicate the percentage of cells in that gate for that particular experiment. (**f**) *Tcra* sequences of fat-derived T_{reg} and T_{conv} cells. Abdominal fat and lymph node T_{reg} and T_{conv} cells were isolated from aged male mice from the LTD mouse line. The frequency of the CDR3α sequences was analyzed on a single-cell basis. Depicted is a graphical display of the TCR sequences in a heat-map format from T_{reg} and T_{conv} cells. (**g**) Staining of CD3, CD4, CD8, Foxp3 and the activation markers CD69 and Ly6c in the stromovascular fraction of cells isolated from abdominal adipose tissue, lymph node, liver and lung from retired-breeder B6 mice. Representative dot plots are shown. Numbers on the graph indicate the percentage of cells in that gate for that particular experiment.

quantification (**Fig. 3a,b** and data not shown). The gene expression differences observed in T_{reg} cells isolated from the fat versus from the spleen and lymph node were not a simple reflection of differing activation statuses, as we observed clearly divergent transcription patterns in a direct comparison between fat-derived and activated T_{reg} cells (**Supplementary Fig. 1**).

A large number of genes were overexpressed, many of them markedly so, by the $CD4^+Foxp3^+$ T cells residing in abdominal adipose tissue but not by the corresponding population at other sites examined (**Fig. 2e**; listed in **Supplementary Table 1**). Chief amongst these overexpressed genes were those encoding molecules involved in leukocyte migration and extravasation: Gm1960 (an IL-10–inducible CXCR2 ligand[25]), CCR1, CCR2, CCR9, CCL6, integrin α_V, activated leukocyte cell adhesion molecule (Alcam), CXCL2 and CXCL10 (**Fig. 2e**, **Supplementary Table 1** and **Supplementary Fig. 2**). In contrast, some molecules of similar function, for example CCL5 and CXCR3, were underexpressed in the visceral fat T_{reg} cells (**Fig. 2e**). Also noteworthy were the extremely high IL-10 transcript levels in $CD4^+Foxp3^+$

abdominal adipose tissue cells (**Fig. 2e** and **Supplementary Fig. 2**). We estimated a 136-fold augmentation of IL-10 transcripts in fat versus lymph node T_{reg} cells from RT-PCR quantification (**Fig. 3c**); we could also detect the increase by intracellular staining for IL-10 protein in the T_{reg} cells of fat versus spleen and lung (**Fig. 3d**). Notably, pathway analysis suggested that the T_{reg} cells not only produced large amounts of IL-10 but also seemed to be responding to it, as a number of genes downstream of the IL-10 receptor were upregulated in fat T_{reg} cells compared with lymph node T_{reg} cells (**Supplementary Fig. 3a**).

Another set of genes was upregulated specifically in $CD4^+Foxp3^-$ T cells residing in adipose tissue as compared with their lymph node counterparts, but not in spleen versus lymph node (**Fig. 2e**; listed in **Supplementary Table 1**). Some of these loci also coded for molecules implicated in migration and extravasation, including CXCR3 and CCL5. Fat-resident T_{conv} cells seemed to be highly polarized to a T helper type 1 phenotype, as they expressed high levels of T-box 21 (Tbet) and interferon-γ (IFN-γ) transcripts (**Fig. 2e**, **Fig. 3c** and
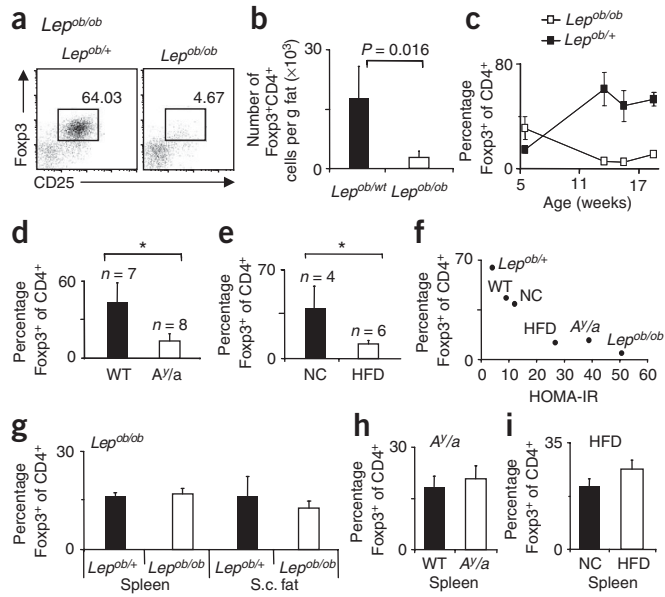
Figure 4 Analysis of fat T_{reg} cells in three mouse models of obesity: $Lep^{ob/ob}$, A^y/a and HFD. (a–c) Abdominal adipose tissue from $Lep^{ob/ob}$ and heterozygote $Lep^{ob/+}$ mice was analyzed for T_{reg} cell frequency. (a) Representative dot plots of $CD4^+$ T cells from 13-week-old mice. (b) Total number of T_{reg} cells per gram of fat. Means ± s.d. are shown. *$P = 0.016$. (c) Changes of T_{reg} cell representation over time. Means ± s.d. are shown. (d) Percentage of T_{reg} cells in abdominal adipose tissue of 24-week-old A^y/a or littermate (WT) mice. *$P = 0.0018$. (e) Percentage of fat T_{reg} cells in mice fed for 29 weeks with HFD or normal chow (NC). *$P = 0.0604$. (f) Correlation of homeostasis model assessment of insulin resistance (HOMA-IR) and fraction of T_{reg} cells. (g–i) Percentage of T_{reg} cells in the spleen and subcutaneous fat in $Lep^{ob/ob}$ (g), A^y/a (h) and HFD-fed mice (i).

Supplementary Fig. 2), abundant intracellular IFN-γ and TNF-α (**Fig. 3d,e**), and little, if any, intracellular IL-4 (**Fig. 3d**). Although the IL-10 effect could also be discerned with fat-resident T_{conv} cells, it was not as striking (**Supplementary Fig. 3b,c**).

Fat-resident T_{reg} cells have a specific T cell receptor repertoire

The T cell receptor (TCR) repertoire is another useful parameter for assessing the degree of similarity of T cell populations. For example, it has been shown that T_{reg} and T_{conv} cell populations have distinct repertoires, with only limited overlap[26–28]. In addition, the TCR repertoire of T_{reg} cells in the abdominal adipose tissue might give an indication of whether their abundance reflects an influx and/or a retention of cells of a particular specificity or a local cytokine-induced conversion[29]. To render the repertoire analysis more manageable and interpretable, we exploited the Limited (LTD) mouse line, wherein TCR diversity is restricted to the complementarity-determining region 3α (CDR3α) via the combination of a transgenic *Tcra* minilocus and the *Tcra*-knockout mutation[30]. We determined CDR3α sequences from 98 individually sorted visceral fat $CD4^+CD25^+$ cells that also expressed Foxp3 RNA, and we compared their distribution with that of CDR3α sequences from fat T_{conv} cells or lymph node T_{reg} and T_{conv} cells. Unfortunately, we were unable to obtain enough T_{reg} cells from subcutaneous fat to perform a parallel TCR sequence analysis on this depot.

As expected, the heat maps generated from these sequences revealed distinct TCR repertoires for the lymph node T_{reg} and T_{conv} cell populations, with only limited overlap (**Fig. 3f**). Similarly, the fat-resident T_{reg} and T_{conv} cell populations also had different repertoires (**Fig. 3f**), rendering it very unlikely that the accumulation of $Foxp3^+$ T_{reg} cells in the abdominal adipose tissue resulted from local conversion of T_{conv} cells. Notably, the fat-resident T_{reg} cells had a very restricted distribution of sequences, representing a distinct subset of those normally found in their lymph node T_{reg} cell counterparts (**Fig. 3f** and **Supplementary Table 2**). The CDR3α sequences characteristic of fat-resident T_{reg} cells were often independently generated by different nucleotide sequences; 50% of sequences (three of six) found more than three times per individual mouse showed such nucleotide variation (**Supplementary Table 3**). In contrast, none of the sequences (zero of ten) from fat-resident T_{conv} cells did (**Supplementary Table 4**), suggesting

the repeated selection of T_{reg} cells with similar antigen receptors rather than the proliferation of a single clone. The sequences were reproducibly frequent in thee different mice, again pointing to TCR-driven selection (**Supplementary Table 3**). These data indicate that the specificity of the TCR may be instrumental in generating the high frequency of T_{reg} cells in visceral fat, perhaps through local recognition of a cognate antigen.

Indeed, fat-resident T_{reg} cells showed unusually high expression of the early activation markers CD69 and lymphocyte antigen 6 complex, locus C1 (Ly6c) (**Fig. 3g**), although it remains possible that such increases instead, or also, reflect cytokine influences. Though TGF-β is readily detectable in adipose tissue[31] and is known to promote T_{reg} cell differentiation and survival[32–34], its effects are an unlikely explanation for the high representation and activation state of T_{reg} cells in fat, because we did not observe the typical changes in gene expression promoted by this growth factor in this population (**Supplementary Fig. 4**). For example, CD103 was not upregulated (**Fig. 2d** and **Fig. 3b**). This observation also argues against TGF-β–mediated conversion of $CD4^+Foxp3^-$ cells to $CD4^+Foxp3^+$ cells in visceral fat, as has been observed in a few systems[29].

Implication of fat-resident T_{reg} cells in metabolic control

To learn how this unique population of T_{reg} cells responds to excess adiposity, we examined it in three mouse models of obesity: leptin-deficient mice ($Lep^{ob/ob}$; commonly referred to as *ob/ob*)[35], mice heterozygous for the yellow spontaneous mutation (A^y/a)[36] and mice chronically fed a high-fat diet (HFD)[3], all on the B6 genetic background and all showing insulin resistance (**Supplementary Fig. 5**). Notably, the T_{reg} cell population in abdominal fat was markedly reduced in aged *ob/ob* mice compared with heterozygous littermates, whether we quantified the fraction of T_{reg} cells in the $CD4^+$ compartment or the number of T_{reg} cells per gram of fat (**Fig. 4a,b**). Whereas 5-week-old leptin-deficient mice had somewhat higher ($P = 0.02$) numbers of $CD4^+Foxp3^+$ T cells in visceral fat (30%) than did wild-type age-matched littermates (10%), this subset progressively declined in the mutant mice and rose in the control mice (**Fig. 4c**) ($P = 0.0011$). As anticipated, *ob/ob* fat-resident T_{reg} cells were relatively depleted among IL-10 producers (**Supplementary Fig. 6a**). The normal proportions of T_{reg} cells in the spleen and subcutaneous fat of *ob/ob* mice argue that the relative scarcity of this subset in visceral fat was not just a reflection of the leptin deficiency; indeed, the absence of this hormone was recently reported to foster the proliferation of T_{reg} cells[37]. Numbers of conventional $CD4^+$ T cells in the abdominal fat of *ob/ob* adults were only mildly lower, and the percentage of these cells making IFN-γ remained essentially unchanged (**Supplementary Fig. 6b,c**).

There were also low proportions of $CD4^+Foxp3^+$ cells in abdominal fat, but not at other sites, in the A^y/a mice and in HFD-fed mice (**Fig. 4d–i**). These low frequencies were not as striking as for *ob/ob* mice (**Fig. 4a**), consistent with less insulin resistance in the latter two

models (**Supplementary Fig. 5**). Indeed, we saw a good correlation between insulin resistance and the fraction of T_{reg} cells in abdominal fat (**Fig. 4f**).

The observed correlation between obesity and insulin resistance on the one hand and a dearth of CD4$^+$Foxp3$^+$ cells in abdominal adipose tissue on the other hand suggests that T_{reg} cells might be implicated in the relationship between the inflammatory and metabolic parameters. To test this notion, we first attempted loss-of-function experiments. Given that it is not currently feasible to ablate T_{reg} cells specifically in fat, we used mice expressing the diphtheria toxin receptor (DTR) under the control of *Foxp3* transcriptional regulatory elements, wherein administration of diphtheria toxin results in rapid systemic

depletion of T_{reg} cells. We recently developed a line of bacterial artificial chromosome (BAC)-transgenic nonobese diabetic (NOD) mice expressing a DTR-eGFP fusion protein under the control of *Foxp3* transcriptional regulatory elements. Routinely, 85–90% of T_{reg} cells are eliminated in the spleen and lymph nodes 2 d after diphtheria toxin administration to these mice (M.F., D. Littman, C.B. and D.M., unpublished data), similar to what has been described by another group with their independently derived line[38].

Cell death induced by diphtheria toxin is apoptotic and therefore does not set off a proinflammatory immune response[39–42], prompting widespread use of this approach to probe diverse immunological issues through specific ablation of particular cell types, including T_{reg}
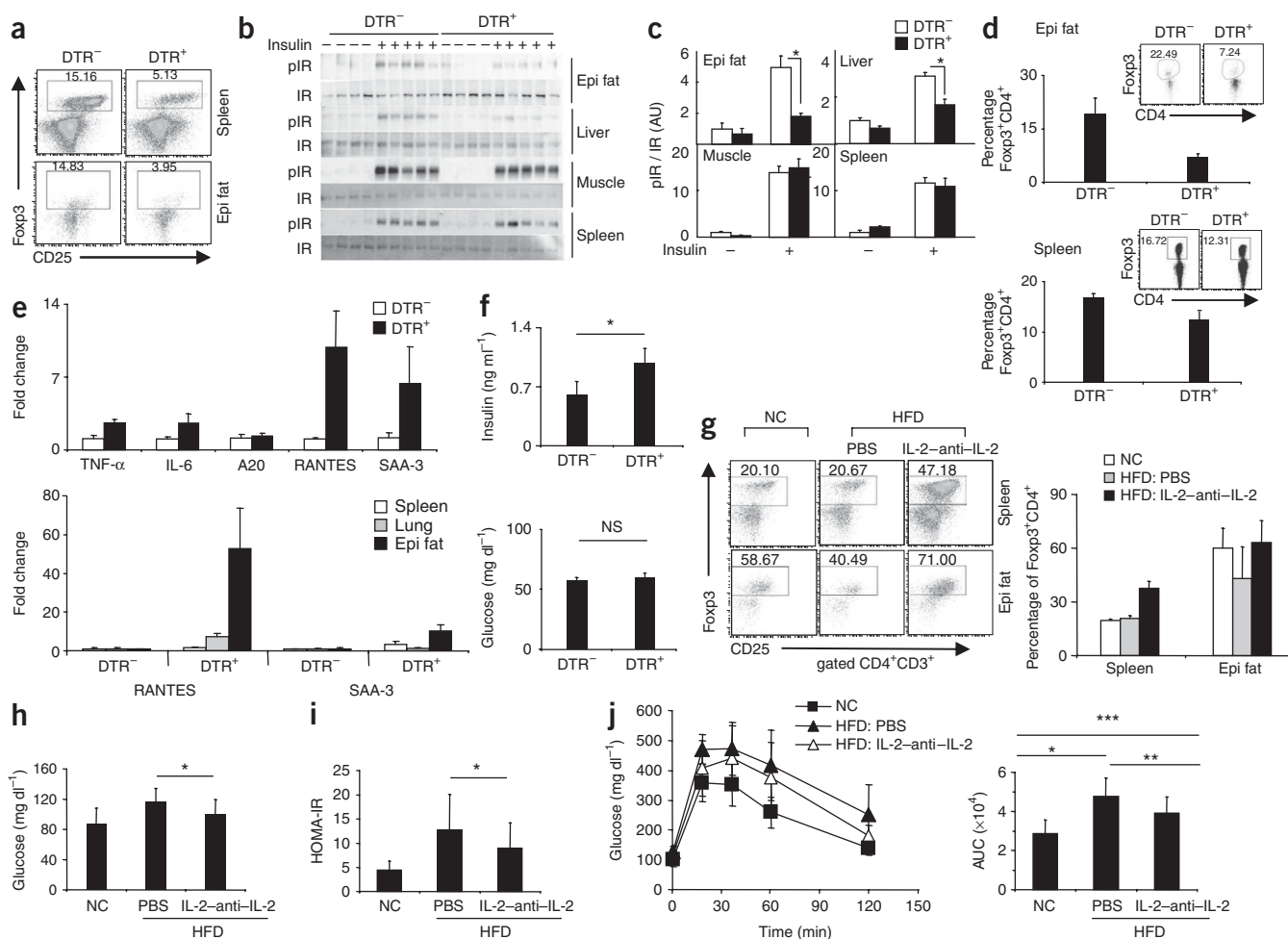
Figure 5 Changes in inflammatory mediators and metabolic parameters in loss- and gain-of-function experiments. (**a–f**) Loss-of-function experiment by depleting T_{reg} cells expressing DTR. 10-week-old male mice, either DTR-positive or DTR-negative, were treated every other day for 4 d (**a–c**) or 9 d (**d–f**) with diphtheria toxin. (**a**) Percentage of T_{reg} cells from spleen or the abdominal fat (Epi fat) after 4 d of treatment. (**b,c**) Insulin signaling in epididymal white adipose tissue (WAT), liver muscle and spleen, as indicated by immunoprecipitation and western blotting of insulin-induced insulin receptor phosphorylation (pIR) (**b**) Blot data. (**c**) Quantification of pIR normalized by total IR ($n \geq 4$, *$P < 0.004$, t test). AU, arbitrary units. (**d**) Percentage of T_{reg} cells from the abdominal fat (top) or spleen (bottom) after 9 d of treatment, with a representative dot plot as an inset. (**e**) Top, expression of TNF-α, IL-6, A20, RANTES and SAA-3 transcripts in abdominal adipose tissue. Three mice per group, one of two independent experiments is shown. Bottom, comparison of RANTES and SAA-3 transcripts in spleen, lung and abdominal fat (epi fat). (**f**) Fasting insulin (top) and fasting glucose (bottom) concentrations after 9 d of treatment every other day. Six mice per group from two independent experiments. *$P = 0.026$. Significance was determined by the Mann-Whitney U test. (**g–j**) Gain-of-function experiment. (**g**) Dot plots (left) and a summarizing bar graph (right) showing T_{reg} cells from spleen and abdominal fat tissue (epi fat) from mice fed normal chow (NC) or with 15 weeks of HFD. Mice were treated with IL-2–IL-2–specific mAb (anti–IL-2) complex or saline for 6 d and analyzed on day 14 ($n = 6$ for each group). Numbers on the graphs indicate the percentage of cells in that gate for that particular experiment. Blood glucose (**h**) HOMA-IR (*$P = 0.078$) (**i**) and an intraperitoneal GTT (*$P = 0.025$) (**j**) of the mice described in **g** are shown. (**j**) Right, calculated area under the curve (AUC) from all mice tested by GTT ($n = 11$ in each group), including the data set described in **g**. *$P = 0.00003$, **$P = 0.036$, ***$P = 0.004$. P values were calculated with the t test. Error bars in all panels represent the means ± s.d.
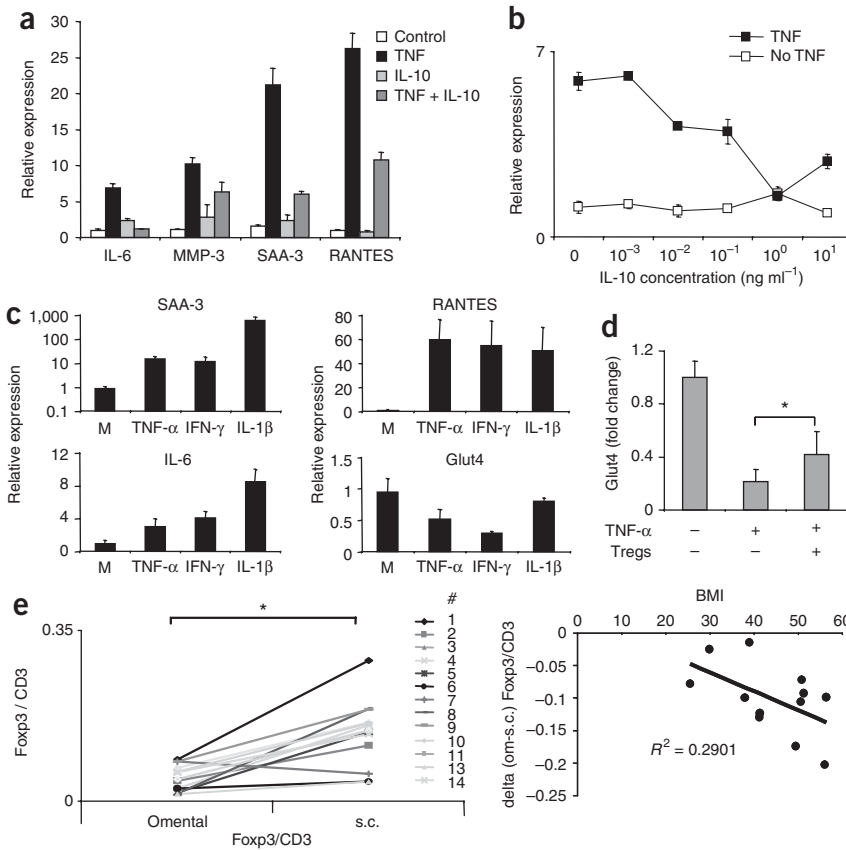
Figure 6 Cytokine effects on adipocytes and human correlates. (**a**) Expression of IL-6, MMP-3, SAA-3 and RANTES, as measured with quantitative PCR under unmanipulated culture conditions (control); adipocytes were treated with TNF-α (TNF), IL-10 (IL-10) alone or TNF-α and IL-10 (TNF + IL-10). (**b**) Relative expression of IL-6 in differentiated adipocytes, dose response curve of IL-10. TNF, cells treated with TNF-α and various concentrations of IL-10. No TNF, cells treated only with IL-10. Representative experiments are shown. (**c**) Expression of SAA-3, RANTES, IL-6 and Glut4 in differentiated adipocytes, unmanipulated differentiated adipocytes (M) or adipocytes treated with TNF-α, IFN-γ and IL-1β. Representative experiments are shown. (**d**) Expression of Glut4 in differentiated adipocytes either unmanipulated or treated with TNF-α in presence or absence of spleen T_{reg} cells. Mean ± s.d. of three independent experiments are shown. *$P = 0.0160$. P value was calculated with t test. (**e**) Paired human omental and subcutaneous adipose samples from mostly obese individuals (BMI range: 25.5–56.43, average: 44.85). Expression of FOXP3 and CD3 was measured by quantitative PCR. Left, the ratios of FOXP3 versus CD3 for omental and subcutaneous adipose tissue. Right, the decrease in FOXP3/CD3 ratio in omental (om) versus subcutaneous adipose tissue plotted against the BMI for each individual donor from the left graph. The positive value of subject 7 (>2 s.d. from the mean) was not included. Each dot represents an individual donor. *$P = 0.000186$. Error bars represent means ± s.d.

cells[39,43–45]. However, because T_{reg} cell–ablated mice develop multi-organ autoimmunity 2 weeks after diphtheria toxin treatment[38], this strategy required us to look at early indicators of potential T_{reg} cell function, namely alterations in adipose tissue RNAs encoding inflammatory mediators or upstream changes in metabolic signaling pathways; previous data suggested that 2 weeks may be too early to see changes in more downstream metabolic parameters, including performance in glucose tolerance tests (GTTs)[46].

For one set of experiments, we treated 10-week-old male mice with diphtheria toxin every other day for 4 d, which lowered the T_{reg} cell level in abdominal fat to about one-fourth the normal level (**Fig. 5a**), whereas the spleen and lung populations were at about one-third the usual level (**Fig. 5a** and data not shown). The depletion of T_{reg} cells was accompanied by substantial decreases in insulin-stimulated insulin receptor tyrosine phosphorylation in epididymal fat and liver, but not in muscle and spleen (**Fig. 5b,c**). We obtained parallel results on AKT protein kinase phosphorylation (data not shown). At this early time point, *in vivo* metabolic changes were marginal (not shown), so we conducted a second set of experiments in which we treated mice with diphtheria toxin for longer times. Mice injected every other day for 9 d had a T_{reg} cell fraction about 30% the usual size of that in the fat, whereas the spleen, lung and lymph node populations had bounced back to about 70% of normal (**Fig. 5d**). We do not know why there is such a preferential loss of T_{reg} cells in adipose tissue with this protocol, but it is likely to reflect slower repopulation kinetics. Concomitantly, many of the genes encoding inflammatory mediators (for example, TNF-α, IL-6, RANTES and serum amyloid A-3 (SAA-3)) were induced in the visceral fat depot (**Fig. 5e**) but much less so in the spleen and lung (**Fig. 5e**). Insulin amounts were significantly higher in the T_{reg} cell-depleted mice, indicating insulin resistance

(**Fig. 5f**), although fasting blood glucose concentrations at this early time point were unchanged, consistent with adequate beta cell compensation (**Fig. 5f**).

To provide additional evidence that the inflammation promoted by T_{reg} cell depletion in the abdominal adipose tissue was not merely a response to cell death, we used mice[38] in which we rapidly ablated T_{reg} cells by giving diphtheria toxin to females carrying a gene encoding DTR knocked into the *Foxp3* locus on the X chromosome. This strategy yielded 95% ablation in homozygous mice versus about 50% ablation in heterozygous mice (**Supplementary Fig. 7**). In the latter case, random X chromosome inactivation protects about half of the T_{reg} cells because the DTR-carrying allele resides within the inactivated chromosome. As expected, when most of the T_{reg} cells were ablated, proinflammatory transcripts (for example, RANTES and MCP-1) were strongly induced in the fat tissue (**Supplementary Fig. 7**). In contrast, when only half the T cells were killed, there was no such induction of proinflammatory transcripts, signifying that substantial diphtheria toxin–induced cell death was not in and of itself the stimulus and that a half-complement of T_{reg} cells sufficed to protect the fat from inflammation.

A gain-of-function experiment involving transfer of fat-resident T_{reg} cells into a recipient fed a high-fat diet could potentially add further support for our proposal that these cells are key mediators of metabolic regulation. However, the lability and low recoverable numbers of visceral fat–resident T_{reg} cells rendered our many attempts at this approach unsuccessful; transfer of more limited numbers of fat-derived T_{reg} cells into lymphodeficient recipients also proved problematic because the resultant homeostatic proliferation altered the phenotype of the introduced population, notably its profile of cell-surface homing receptors (data not shown). Therefore, as an

alternative means to achieve gain-of-function, we turned to *in situ* expansion of T_{reg} cells via injection of a complex consisting of recombinant IL-2 and a particular–IL-2–specific monoclonal antibody (mAb), previously shown to selectively elicit T_{reg} cells[47,48]. Daily injections of the complex for 6 d into mice prefed on HFD for 15 weeks did substantially increase the fraction of T_{reg} cells in the spleen and abdominal fat as compared with PBS-injected controls (averages from multiple experiments 37% ± 4% versus 21% ± 2% for spleen and 63% ± 12% versus 43% ± 17% for abdominal fat; **Fig. 5g**). (The reduction in the T_{reg} cell fraction in PBS-injected HFD-fed mice versus mice fed normal chow is smaller in **Fig. 5** than in **Fig. 4** because of the shorter time of HFD.)

To assess insulin resistance in the complex-injected mice, we measured blood glucose concentrations, which were significantly lower (**Fig. 5h**). As expected, IL-10 transcript levels were significantly higher in the HFD-fed mice with more T_{reg} cells (**Supplementary Fig. 6d**). Whereas HOMA-IR (a standard measure of insulin resistance that integrates both blood-glucose and blood-insulin concentrations; **Fig. 5i**) and glucose tolerance (measured via an intraperitoneal GTT; **Fig. 5j**) all trended toward lower values in the T_{reg} cell–enriched, HFD-fed mice, these differences fell short of statistical significance, probably owing to the greater experimental variability inherent in these assays. In fact, given the very short experimental window that we had to work in to avoid expansion of effector T cells, we do not find small differences at all surprising. To enhance the power of the experimental data, we injected a number of additional HFD-fed mice with the IL-2–based complexes or PBS under similar conditions, accumulating a total of 11 mice for each group. The T_{reg} cell fraction in the complex-injected, HFD-fed mice ranged from 40% to 83% (average 68% ± 13%), whereas that in the PBS-injected mice spanned 18% to 70% (average 45% ± 13%). Both HFD-fed groups were glucose intolerant as compared with control mice fed normal chow; however, the complex-injected group, with the highest levels of T_{reg} cells, showed a significant improvement compared with the PBS-injected group (**Fig. 5j**). We obtained similar results in the A^y/a model (**Supplementary Fig. 8**).

Together, the loss-of-function and gain-of-function findings indicate that T_{reg} cells guard against excessive inflammation of the adipose tissue and its downstream systemic consequences and strongly suggest that T_{reg} cells residing in the fat are responsible.

In vitro effects of T cell-derived cytokines on adipocytes

A probable mechanism by which T cells residing in adipose tissue affect neighboring cells is through soluble mediators. Thus, we explored the influences of the major cytokines differentially produced by T_{reg} and T_{conv} cells in fat versus other tissues (IL-10 and IFN-γ, respectively; **Fig. 2**). We pretreated fully differentiated, lipid-laden 3T3-L1 adipocytes for 48 h with IL-10 (or left them untreated) and subsequently stimulated them for 24 h with TNF-α, an established method for *in vitro* induction of insulin resistance. TNF-α induced changes in adipocyte expression of a number of transcripts encoding inflammatory mediators, for example IL-6, RANTES, SAA-3 and MMP-3; of note, IL-10 inhibited the TNF-α-induced expression of all of these RNAs (**Fig. 6a,b**). TNF-α has also been shown to downmodulate insulin-dependent tyrosine phosphorylation of insulin receptor substrate-1 and to inhibit glucose uptake mediated by the glucose transporter Glut4 in 3T3-L1 adipocytes; these effects, too, were reversed by IL-10 (ref. 8), indicating that this cytokine reverts insulin resistance by a mechanism directly impinging on adipose tissue cells. In contrast to the anti-inflammatory effects of IL-10 made by visceral fat-resident T_{reg} cells, a major product of the T_{conv} cells at this site,

IFN-γ, was proinflammatory in the same *in vitro* assay system, as expression of SAA-3, RANTES and IL-6 transcripts was induced, and Glut4 RNA was downregulated (**Fig. 6c**).

Our many attempts to support these conclusions by performing cocultures of fat-derived T_{reg} cells and 3T3-L1 preadipocytes have so far been unsuccessful owing to rapid death of the T_{reg} cells during the incubation period, probably as a result of proapoptotic factors either in the medium or produced by the adipocytes, such as TNF-α. However, spleen T_{reg} cells were less fragile in these coculture conditions, and we could show that they dampen levels of proinflammatory transcripts made by activated adipocytes in culture and, perhaps most relevant, inhibit their downmodulation of Glut-4 transcripts (**Fig. 6d** and data not shown). The greater fragility of fat-derived versus spleen-derived T_{reg} cells may be explained by the former cells' higher expression of TNF receptors (data not shown).

FOXP3 transcripts are reduced in obese human omental fat

Finally, we sought to translate our findings to human pathology. We had access to a set of paired frozen omental and subcutaneous fat tissues from a number of individuals with an average body mass index (BMI) of 44.85, thus (except for one case) falling within the obese (30–39.9) and morbidly obese (>40) range (human subject characteristics given in **Supplementary Table 5**). Given that the samples were frozen, we could not perform flow cytometric analysis on or purification of lymphocyte populations, but we could determine *FOXP3* transcript levels by PCR. FOXP3 RNA was readily detectable in both fat depots (**Fig. 6e**). Consistent with the observations on obese mice, we found higher levels of FOXP3 transcripts, presumably an indicator of T_{reg} cells, in the subcutaneous adipose tissue (**Fig. 6e**). We did not have access to nonobese controls for these studies, owing to the rarity of bariatric surgery on normal individuals. However, we did find a correlation between BMI and the drop in T_{reg} cells in omental versus subcutaneous fat (**Fig. 6e**). These data suggest that our findings on mice may be translatable to humans, which is encouraging for future, more sophisticated analyses on purified T cell subsets from fresh adipose tissue.

DISCUSSION

Finding what appears to be a unique population of regulatory T lymphocytes enriched in the abdominal adipose tissue of normal, but not obese, mice raises a number of questions. First, why and how do T_{reg} cells accumulate at this site? One factor may be antigen stimulation, as suggested by the imprint of antigenic selection on the TCR repertoire of visceral fat T_{reg} cells and by their unusually high state of activation. Depending on the location of any such antigens, they could stimulate circulating T_{reg} cells, provoking them to exit the lymph nodes and invade the fat and/or restimulate T_{reg} cells filtering through adipose tissue, thereby promoting their retention. This notion is further supported by the sequencing and the gene-expression profiling data, which rule out the possibility that T_{conv} cells are induced to convert to T_{reg} cells in the visceral fat. A second factor is almost certainly chemokines, given the unique pattern of chemokine–chemokine receptor gene expression by the T_{reg} cells isolated from adipose tissue. Functional studies will be needed to unravel which of these molecules are indeed involved in cell attraction or access to fat, their localization once therein or their recruitment of other leukocyte subsets. Third, there may be a role for adipokines in nurturing T_{reg} cell survival in adipose tissue. A recent study highlighted the negative effect of leptin on the proliferative capacity of T_{reg} cells[37], which fits well with their opposite proportions in normal and obese fat: many T_{reg} cells and little leptin in lean fat tissue and few T_{reg} cells and much

leptin in obese fat. In contrast, given the parallel high levels of T_{reg} cells and adiponectin in normal fat and low levels in obese fat, this adipokine is a possible candidate for a positive factor, especially as it induces IL-10 synthesis, at least by macrophages[49,50].

Next, what function are T_{reg} cells performing in normal abdominal adipose tissue? Recent reports have highlighted the interplay between adipocytes and a population of anti-inflammatory macrophages in this fat depot, suggesting a role for resident macrophages in promoting tissue repair and angiogenesis and in maintaining insulin sensitivity[8,9]. Our results argue that the activities of coincident populations of T_{conv} and T_{reg} cells need to be added to the mix. It may be relevant that the T_{conv} cells seem to be making an ongoing T helper type 1 response to some stimulus and that their major product, IFN-γ, promotes synthesis of inflammatory mediators by adipocytes. The T_{reg} cells may be keeping this response in check, as well as regulating the activities of their macrophage and adipocyte neighbors—indeed, their physical location in crown-like structures at adipocyte junctions would encourage interaction with both cell types. IL-10 is one candidate for having a role in T_{reg} cell–mediated regulatory activities, given its association with improved insulin sensitivity in a number of contexts in both rodents and humans[51–53], although this cytokine is also produced by the fat-resident anti-inflammatory macrophages[8]. Although it was not feasible to more definitively establish the specific function of T_{reg} cells residing in adipose tissue, given that no fat-resident T_{reg} cell–specific reagent exists and that it has not been possible to successfully isolate and transfer fat-derived T_{reg} cells in the requisite quantities, a role for T_{reg} cells, whatever their source, in metabolic homeostasis and its dysregulation in obesity is an unexpected finding.

Lastly, what provokes T_{reg} cells to vacate abdominal fat in obesity, or, perhaps more likely, to refrain from entering it? It may be a secondary effect. Increasing adiposity has been associated with an influx of macrophages[6,7], in particular the inflammatory macrophage subset[8,9], into the abdominal depot; as well as with increased local and systemic concentrations of inflammatory cytokines such as TNF-α and IL-6. In addition, a reciprocal increase and decrease in the adipokines leptin and adiponectin, respectively, has been reported, fueling speculation of extensive crosstalk between the two cell types in the obese condition[11]. One possible scenario, then, is that elements of this changing environment are unfavorable for T_{reg} cell entry, expansion or survival, leading to a secondary decline of this regulatory population; in fact, leptin[37] and IL-6 (refs. 54,55) are already known to have such properties. However, it is also possible that loss of T_{reg} cells from the abdominal fat is the primary effect. Whereas their exaggerated numbers in lean adipose tissue may have been sufficient to keep the chronic inflammation under control, lower T_{reg} cell numbers with increasing adiposity could open the gate to an invasion of inflammatory macrophages and thereby a more robust synthesis of inflammatory cytokines. Whether the influx of macrophages or the efflux (or death) of T_{reg} cells proves upstream, both processes must be downstream of an initiating event, as yet undefined, though suggestions have included local hypoxia[56], increased adipocyte death[20] and adipocyte stress[57].

METHODS

Methods and any associated references are available in the online version of the paper at http://www.nature.com/naturemedicine/.

Accession codes. Microarray data have been deposited in the Gene Expression Omnibus with accession code GSE7852.

Note: Supplementary information is available on the Nature Medicine website.

1. Shoelson, S.E., Lee, J. & Goldfine, A.B. Inflammation and insulin resistance. *J. Clin. Invest.* **116**, 1793–1801 (2006).
2. Hotamisligil, G.S., Shargill, N.S. & Spiegelman, B.M. Adipose expression of tumor necrosis factor-α: direct role in obesity-linked insulin resistance. *Science* **259**, 87–91 (1993).
3. Cai, D. *et al.* Local and systemic insulin resistance resulting from hepatic activation of IKKβ and NF-κB. *Nat. Med.* **11**, 183–190 (2005).
4. Bosello, O. & Zamboni, M. Visceral obesity and metabolic syndrome. *Obes. Rev.* **1**, 47–56 (2000).
5. Fantuzzi, G. Adipose tissue, adipokines and inflammation. *J. Allergy Clin. Immunol.* **115**, 911–919 (2005).
6. Weisberg, S.P. *et al.* Obesity is associated with macrophage accumulation in adipose tissue. *J. Clin. Invest.* **112**, 1796–1808 (2003).
7. Xu, H. *et al.* Chronic inflammation in fat plays a crucial role in the development of obesity-related insulin resistance. *J. Clin. Invest.* **112**, 1821–1830 (2003).
8. Lumeng, C.N., Bodzin, J.L. & Saltiel, A.R. Obesity induces a phenotypic switch in adipose tissue macrophage polarization. *J. Clin. Invest.* **117**, 175–184 (2007).
9. Lumeng, C.N., Deyoung, S.M., Bodzin, J.L. & Saltiel, A.R. Increased inflammatory properties of adipose tissue macrophages recruited during diet-induced obesity. *Diabetes* **56**, 16–23 (2007).
10. Odegaard, J.I. *et al.* Macrophage-specific PPARgamma controls alternative activation and improves insulin resistance. *Nature* **447**, 1116–1120 (2007).
11. Suganami, T., Nishida, J. & Ogawa, Y. A paracrine loop between adipocytes and macrophages aggravates inflammatory changes: role of free fatty acids and tumor necrosis factor α. *Arterioscler. Thromb. Vasc. Biol.* **25**, 2062–2068 (2005).
12. Caspar-Bauguil, S. *et al.* Adipose tissues as an ancestral immune organ: site-specific change in obesity. *FEBS Lett.* **579**, 3487–3492 (2005).
13. Zheng, Y. & Rudensky, A.Y. Foxp3 in control of the regulatory T cell lineage. *Nat. Immunol.* **8**, 457–462 (2007).
14. Sakaguchi, S., Yamaguchi, T., Nomura, T. & Ono, M. Regulatory T cells and immune tolerance. *Cell* **133**, 775–787 (2008).
15. Maloy, K.J. *et al.* CD4+CD25+ T_R cells suppress innate immune pathology through cytokine-dependent mechanisms. *J. Exp. Med.* **197**, 111–119 (2003).
16. Murphy, T.J., Choileain, N.N., Zang, Y., Mannick, J.A. & Lederer, J.A. CD4+CD25+ regulatory T cells control innate immune reactivity after injury. *J. Immunol.* **174**, 2957–2963 (2005).
17. Nguyen, L.T., Jacobs, J., Mathis, D. & Benoist, C. Where FoxP3-dependent regulatory T cells impinge on the development of inflammatory arthritis. *Arthritis Rheum.* **56**, 509–520 (2007).
18. Wu, H. *et al.* T-cell accumulation and regulated on activation, normal T cell expressed and secreted upregulation in adipose tissue in obesity. *Circulation* **115**, 1029–1038 (2007).
19. Tran, T.T., Yamamoto, Y., Gesta, S. & Kahn, C.R. Beneficial effects of subcutaneous fat transplantation on metabolism. *Cell Metab.* **7**, 410–420 (2008).
20. Cinti, S. *et al.* Adipocyte death defines macrophage localization and function in adipose tissue of obese mice and humans. *J. Lipid Res.* **46**, 2347–2355 (2005).
21. Fontenot, J.D. *et al.* Regulatory T cell lineage specification by the forkhead transcription factor Foxp3. *Immunity* **22**, 329–341 (2005).
22. Huehn, J. *et al.* Developmental stage, phenotype, and migration distinguish naive- and effector/memory-like CD4+ regulatory T cells. *J. Exp. Med.* **199**, 303–313 (2004).
23. Herman, A.E., Freeman, G.J., Mathis, D. & Benoist, C. CD4+CD25+ T regulatory cells dependent on ICOS promote regulation of effector cells in the prediabetic lesion. *J. Exp. Med.* **199**, 1479–1489 (2004).
24. Hill, J. *et al.* Foxp3-transcription-factor–dependent and –independent regulation of the regulatory T cell transcriptional signature. *Immunity* **27**, 786–800 (2007).
25. Nolan, K.F. *et al.* IL-10–conditioned dendritic cells, decommissioned for recruitment of adaptive immunity, elicit innate inflammatory gene products in response to danger signals. *J. Immunol.* **172**, 2201–2209 (2004).

26. Wong, J. et al. Adaptation of TCR repertoires to self-peptides in regulatory and nonregulatory CD4+ T cells. J. Immunol. **178**, 7032–7041 (2007).
27. Hsieh, C.S., Zheng, Y., Liang, Y., Fontenot, J.D. & Rudensky, A.Y. An intersection between the self-reactive regulatory and nonregulatory T cell receptor repertoires. Nat. Immunol. **7**, 401–410 (2006).
28. Pacholczyk, R., Ignatowicz, H., Kraj, P. & Ignatowicz, L. Origin and T cell receptor diversity of Foxp3+CD4+CD25+ T cells. Immunity **25**, 249–259 (2006).
29. Kretschmer, K. et al. Inducing and expanding regulatory T cell populations by foreign antigen. Nat. Immunol. **6**, 1219–1227 (2005).
30. Correia-Neves, M., Waltzinger, C., Mathis, D. & Benoist, C. The shaping of the T cell repertoire. Immunity **14**, 21–32 (2001).
31. Samad, F., Yamamoto, K., Pandey, M. & Loskutoff, D.J. Elevated expression of transforming growth factor-β in adipose tissue from obese mice. Mol. Med. **3**, 37–48 (1997).
32. Chen, W. et al. Conversion of peripheral CD4+CD25− naive T cells to CD4+CD25+ regulatory T cells by TGF-β induction of transcription factor Foxp3. J. Exp. Med. **198**, 1875–1886 (2003).
33. Peng, Y., Laouar, Y., Li, M.O., Green, E.A. & Flavell, R.A. TGF-β regulates in vivo expansion of Foxp3-expressing CD4+CD25+ regulatory T cells responsible for protection against diabetes. Proc. Natl. Acad. Sci. USA **101**, 4572–4577 (2004).
34. Marie, J.C., Letterio, J.J., Gavin, M. & Rudensky, A.Y. TGF-β1 maintains suppressor function and Foxp3 expression in CD4+CD25+ regulatory T cells. J. Exp. Med. **201**, 1061–1067 (2005).
35. Pelleymounter, M.A. et al. Effects of the obese gene product on body weight regulation in ob/ob mice. Science **269**, 540–543 (1995).
36. Klebig, M.L., Wilkinson, J.E., Geisler, J.G. & Woychik, R.P. Ectopic expression of the agouti gene in transgenic mice causes obesity, features of type II diabetes and yellow fur. Proc. Natl. Acad. Sci. USA **92**, 4728–4732 (1995).
37. De Rosa, V. et al. A key role of leptin in the control of regulatory T cell proliferation. Immunity **26**, 241–255 (2007).
38. Kim, J.M., Rasmussen, J.P. & Rudensky, A.Y. Regulatory T cells prevent catastrophic autoimmunity throughout the lifespan of mice. Nat. Immunol. **8**, 191–197 (2007).
39. Bennett, C.L. & Clausen, B.E. DC ablation in mice: promises, pitfalls and challenges. Trends Immunol. **28**, 525–531 (2007).
40. Thorburn, J., Frankel, A.E. & Thorburn, A. Apoptosis by leukemia cell–targeted diphtheria toxin occurs via receptor-independent activation of Fas-associated death domain protein. Clin. Cancer Res. **9**, 861–865 (2003).
41. Miyake, Y. et al. Protective role of macrophages in noninflammatory lung injury caused by selective ablation of alveolar epithelial type II cells. J. Immunol. **178**, 5001–5009 (2007).
42. Bennett, C.L. et al. Inducible ablation of mouse Langerhans cells diminishes but fails to abrogate contact hypersensitivity. J. Cell Biol. **169**, 569–576 (2005).
43. Duffield, J.S. et al. Conditional ablation of macrophages halts progression of crescentic glomerulonephritis. Am. J. Pathol. **167**, 1207–1219 (2005).
44. Duffield, J.S. et al. Selective depletion of macrophages reveals distinct, opposing roles during liver injury and repair. J. Clin. Invest. **115**, 56–65 (2005).
45. Walzer, T. et al. Identification, activation and selective in vivo ablation of mouse NK cells via NKp46. Proc. Natl. Acad. Sci. USA **104**, 3384–3389 (2007).
46. Yuan, M. et al. Reversal of obesity- and diet-induced insulin resistance with salicylates or targeted disruption of Ikkbeta. Science **293**, 1673–1677 (2001).
47. Boyman, O., Kovar, M., Rubinstein, M.P., Surh, C.D. & Sprent, J. Selective stimulation of T cell subsets with antibody-cytokine immune complexes. Science **311**, 1924–1927 (2006).
48. Tang, Q. et al. Central role of defective interleukin-2 production in the triggering of islet autoimmune destruction. Immunity **28**, 687–697 (2008).
49. Wolf, A.M., Wolf, D., Rumpold, H., Enrich, B. & Tilg, H. Adiponectin induces the anti-inflammatory cytokines IL-10 and IL-1RA in human leukocytes. Biochem. Biophys. Res. Commun. **323**, 630–635 (2004).
50. Kumada, M. et al. Adiponectin specifically increased tissue inhibitor of metalloproteinase-1 through interleukin-10 expression in human macrophages. Circulation **109**, 2046–2049 (2004).
51. Kim, H.J. et al. Differential effects of interleukin-6 and -10 on skeletal muscle and liver insulin action in vivo. Diabetes **53**, 1060–1067 (2004).
52. Blüher, M. et al. Association of interleukin-6, C-reactive protein, interleukin-10 and adiponectin plasma concentrations with measures of obesity, insulin sensitivity and glucose metabolism. Exp. Clin. Endocrinol. Diabetes **113**, 534–537 (2005).
53. Scarpelli, D. et al. Variants of the interleukin-10 promoter gene are associated with obesity and insulin resistance but not type 2 diabetes in Caucasian Italian subjects. Diabetes **55**, 1529–1533 (2006).
54. Doganci, A. et al. The IL-6R α chain controls lung CD4+CD25+ Treg development and function during allergic airway inflammation in vivo. J. Clin. Invest. **115**, 313–325 (2005).
55. Wan, S., Xia, C. & Morel, L. IL-6 produced by dendritic cells from lupus-prone mice inhibits CD4+CD25+ T cell regulatory functions. J. Immunol. **178**, 271–279 (2007).
56. Hosogai, N. et al. Adipose tissue hypoxia in obesity and its impact on adipocytokine dysregulation. Diabetes **56**, 901–911 (2007).
57. Furukawa, S. et al. Increased oxidative stress in obesity and its impact on metabolic syndrome. J. Clin. Invest. **114**, 1752–1761 (2004).

ONLINE METHODS

Mice. Male B6 (at various ages and retired breeders 25–35-weeks-old), mice homozygous for the obese spontaneous leptin mutation, ($Lep^{ob/ob}$; commonly referred to as *ob/ob*) and $Lep^{ob/+}$ mice, and mice heterozygous for the yellow spontaneous mutation (A^y/a) were purchased from the Jackson Laboratory. $Foxp3^{GFP}$ B6 reporter mice[21] and LTD mice[30] were bred in our specific pathogen–free facility at the Joslin Diabetes Center. For HFD, we fed the mice with a rodent diet of 45 kcal% or 60 kcal% fat from Research Diet (D12451). Other HFD-fed mice were bought from Jackson Laboratory, as indicated in the **Supplementary Methods**. We generated mice expressing DTR under the control of *Foxp3* regulatory elements ($Foxp3^{DTR}$) on the NOD genetic background, starting with a construct provided by D. Littman. For that construct, a BAC spanning the region from 150 kilobases upstream to 70 kilobases downstream of the *Foxp3* transcription start site was isolated, and a DTR-eGFP cDNA (encoding a fusion protein consisting of eGFP joined to the carboxy-terminus of the human DTR) followed by a stop codon was inserted between the first and second codons of the *Foxp3* open reading frame.

We injected the recombinant Foxp3-DTR-eGFP BAC into NOD fertilized oocytes, and the resulting embryos were implanted into pseudopregnant mothers by standard procedures. We typed offspring for the eGFP insert by PCR, and we mated positive males to NOD mice. Mouse experiments were conducted under protocols approved by the Institutional Animal care and Use Committee of the Joslin Diabetes Center.

Isolation of T cells and cytokine stimulation assay. We removed abdominal (epidydimal) adipose tissue, subcutaneous adipose tissue, lung and liver after flushing the organs through the portal vein and the heart ventricle, cut them into small pieces (or passed them through a sieve in the case of the liver) and digested them for about 40 min with collagenase type II (adipose tissue, Sigma) or collagenase type IV (Sigma). We then filtered the cell suspensions through a sieve (or, for the lung, mashed them through the sieve), and collected the stromovascular fraction after centrifugation. We stained the cells with mAbs specific for CD4, CD8, CD3, CD25 and B220; and, for some experiments, with a mAb specific for CD103, GITR, CD69 or Ly6c. We then fixed and permeabilized the cells according to the manufacturer's instructions (eBiosciences), followed by intracellular staining of Foxp3 (eBiosciences) and CTLA-4 (BD Bioscience).

For intracellular cytokine staining, we stimulated the cells with pokeweed mitogen antigen (50ng ml^{-1}) (Sigma) and ionomycin (1nM) (Calbiochem) for 4 h. We added Golgistop (BD) to the culture at the recommended amount during the last 3 h. We stained cells with mAbs specific for CD4, CD8, CD3, CD25 and B220 and then fixed and permeabilized them according to the manufacturer's instructions (eBiosciences), followed by intracellular staining of Foxp3 (eBiosciences), IFN-γ, TNF-α, IL-10 or IL-4 (all mAbs recognizing cytokines were from BD). We then analyzed the cells were with Moflo, Coulter Epics XL or the Becton Dickinson LSRII instruments, and FlowJo software (Tree Star).

Microarray analysis. We sorted lymph node and abdominal fat TCR$^+$CD4$^+$ and CD25^{hi} (T$_{reg}$) or TCR$^+$CD4$^+$ and CD25$^-$ (T$_{conv}$) cells from retired male breeder B6 mice, and we sorted spleen T$_{reg}$ and T$_{conv}$ cells from Foxp3^{GFP} B6 reporter mice[21]. We extracted RNA with Trizol (Invitrogen) and amplified it for two rounds using the MessageAmp amplified RNA kit (Ambion), followed by biotin labeling with the BioArray High Yield RNA Transcription Labeling Kit (Enzo Diagnostics) and purification with the RNeasy Mini Kit (Qiagen). We hybridized the resulting cRNAs (three independent data sets for each sample type) to M430 2.0 chips (Affymetrix) according to the manufacturer's protocol. We processed initial reads through Affymetrix software to obtain raw .cel files. We background-correct and normalized microarray data with the robust multichip analysis algorithm implemented in the GenePattern software package[58], and we averaged the replicates. We compiled a consensus T$_{reg}$ signature from four independent analyses[23,26]. The fat T$_{reg}$–specific gene set included loci specifically over- or underexpressed in fat T$_{reg}$ cells, and we generated it by including genes twofold or more over- or underexpressed in fat T$_{reg}$ cells versus fat T$_{conv}$ cells, as well as more than twofold different between fat T$_{reg}$ and lymph node T$_{conv}$ cells. To exclude the classical T$_{reg}$-specific genes, the ratio of lymph node T$_{reg}$ versus lymph node T$_{conv}$ values had to be between 1.25 and 0.8. Itgav, integrin α$_5$.

***In vivo* depletion and expansion of Treg cells.** For depletion, we injected 10-week-old Foxp3^{DTR+} mice and Foxp3^{DTR-}control littermates intraperitoneally with diphtheria toxin (Sigma), at 40ng per g body weight, every other day for 9 d or, in some experiments, for 4 d. We measured overnight fasting blood glucose and insulin concentrations, and we removed abdominal adipose tissue, lung and spleen for RNA extraction.

For expansion, we purchased, from Jackson Laboratory, mice fed for 12 weeks on HFD (60 kcal% fat from Research Diet, D12492) and then fed them on the same chow another 3 weeks in our facility. We prepared complexes of the IL-2–specific mAb JES6-5H4 (BD) and recombinant mouse IL-2 (Pepro-Tech) and injected them intraperitoneally as previously described[47]. In brief, we incubated 5 µg of IL-2–specific mAb and 0.5 µg mouse IL-2 per mouse for 20 min on ice followed by intraperitoneal injection. We gave the mice daily injections for 6 or 9 d, and we analyzed them on day 14. We injected control mice with saline (PBS). In some experiments, we fed mice with HFD for 8 weeks (60 kcal% fat from Research Diet, D12492) and injected them with the complex for 9 d. For GTTs, we administered glucose (2.0 g per kg body weight) by intraperitoneal injection after an overnight fast. We measured blood glucose before, 15, 30, 60 and 120 min after glucose application.

Human subjects. We obtained human subcutaneous and omental adipose tissue samples at the time of elective abdominal surgery and immediately froze them until analysis. Samples were obtained with written informed consent and were approved by the Institutional Review Boards of both the Joslin Diabetes Center and Beth Israel Deaconess Medical Center.

Statistical analyses. Data were routinely presented as means ± s.d., and we determined significance by the Student's *t* test or Mann-Whitney *U* test (as indicated). We considered a *P* value of <0.05 as statistically significant.

58. Reich, M. *et al.* GenePattern 2.0. *Nat. Genet.* **38**, 500–501 (2006).